

See discussions, stats, and author profiles for this publication at: <https://www.researchgate.net/publication/51491810>

# Simultaneous Detection of Transgenic DNA by Surface Plasmon Resonance Imaging with Potential Application to Gene Doping Detection

ARTICLE in ANALYTICAL CHEMISTRY · AUGUST 2011

Impact Factor: 5.64 · DOI: 10.1021/ac200877m · Source: PubMed

CITATIONS

11

READS

37

6 AUTHORS, INCLUDING:



**Maria Laura Ermini**

Institute of Photonics and Electronics (IPE)

15 PUBLICATIONS 94 CITATIONS

SEE PROFILE



**Marco Mascini**

University of Florence

395 PUBLICATIONS 11,662 CITATIONS

SEE PROFILE



**Patrizia Bogani**

University of Florence

50 PUBLICATIONS 602 CITATIONS

SEE PROFILE



**Maria Minunni**

University of Florence

111 PUBLICATIONS 3,940 CITATIONS

SEE PROFILE

# Simultaneous Detection of Transgenic DNA by Surface Plasmon Resonance Imaging with Potential Application to Gene Doping Detection

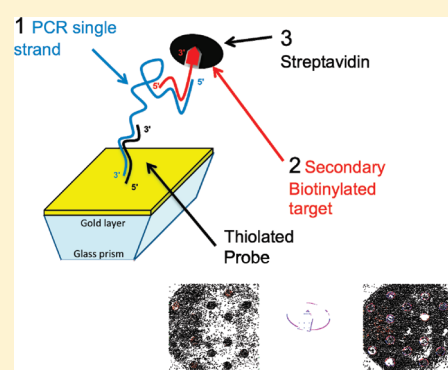
Simona Scarano,<sup>†</sup> Maria Laura Ermini,<sup>†</sup> Maria Michela Spiriti,<sup>‡</sup> Marco Mascini,<sup>†</sup> Patrizia Bogani,<sup>‡</sup> and Maria Minunni<sup>\*,†</sup>

<sup>†</sup>Dipartimento di Chimica, Università degli Studi di Firenze “Ugo Schiff”, 50019 Sesto Fiorentino, Italy

<sup>‡</sup>Dipartimento di Biologia Evoluzionistica “Leo Pardi”, Università degli Studi di Firenze, 50127 Firenze, Italy

**S** Supporting Information

**ABSTRACT:** Surface plasmon resonance imaging (SPRi) was used as the transduction principle for the development of optical-based sensing for transgenes detection in human cell lines. The objective was to develop a multianalyte, label-free, and real-time approach for DNA sequences that are identified as markers of transgenesis events. The strategy exploits SPRi sensing to detect the transgenic event by targeting selected marker sequences, which are present on shuttle vector backbone used to carry out the transfection of human embryonic kidney (HEK) cell lines. Here, we identified DNA sequences belonging to the *Cytomegalovirus* promoter and the Enhanced Green Fluorescent Protein gene. System development is discussed in terms of probe efficiency and influence of secondary structures on biorecognition reaction on sensor; moreover, optimization of PCR samples pretreatment was carried out to allow hybridization on biosensor, together with an approach to increase SPRi signals by *in situ* mass enhancement. Real-time PCR was also employed as reference technique for marker sequences detection on human HEK cells. We can foresee that the developed system may have potential applications in the field of antidoping research focused on the so-called gene doping.



The World Anti-Doping Agency (WADA) and sports authorities seriously fear that the so-called “gene doping” may soon become a widely used approach to enhance athletic performance. Even though, until now, only few suspects have proliferated on the sports ground, since 2003, WADA began to give serious consideration to the need of analytical methods that are able to detect and unmask this prohibited doping practice. Despite the fact that almost a decade has now passed, we can observe that official methods for gene doping detection are yet to be established. Only recently have such research papers concerning this topic begun to emerge.<sup>1–5</sup> The primary cause of this delay is undoubtedly related to the high complexity of the phenomenon, which is defined as “the transfer of nucleic acids or nucleic acid sequences, the use of normal or genetically modified cells, and/or the use of agents that directly or indirectly affect functions known to influence performance by altering gene expression”. (See [http://www.wada-ama.org/Documents/World\\_Anti-Doping\\_Program/WADP-Prohibited-list/To\\_be\\_effective/WADA\\_Prohibited\\_List\\_2011\\_EN.pdf](http://www.wada-ama.org/Documents/World_Anti-Doping_Program/WADP-Prohibited-list/To_be_effective/WADA_Prohibited_List_2011_EN.pdf)). Different from doping methods and substances utilized in the past, the doping substances are directly produced *in situ* by the athlete’s own cells before exogenous genes with performance-enhancing effects are introduced and expressed directly into the body. We previously discussed the potential application of

affinity-based biosensors (ABBs) in gene doping analysis, also in combination with other analytical technologies.<sup>6</sup> In ABBs, the formation of an affinity complex on the sensing surface is common and it is usually detected with high selectivity, reproducibility, and sensitivity.<sup>7</sup> ABBs are capable of performing an unambiguous identification of target analytes and thus could be used for both direct (transgenes, transgenic elements, and/or recombinant proteins) and indirect (immunoresponse, side-effects on metabolome) gene doping detections. The first successful application was performed by piezoelectric devices and applied to human DNA extracted from transgenic cells samples. The detection strategy proposed was based on a direct yes/no response: the transgenic event was tracked by targeting suitable DNA sequences of the shuttle vector backbone used to carry out the transgenesis protocol (i.e., promoters and marker sequences are used as fingerprint of the underlying gene transfer event). As proof of principle of the biosensor feasibility, a selected transgenic DNA shuttle (plasmid EGFP-C1) was detected after its delivery into Human Embryonic Kidney (HEK) cell lines, in a reproducible and specific manner. These

**Received:** April 6, 2011

**Accepted:** July 14, 2011

**Published:** July 14, 2011

encouraging results stimulated further development of the affinity-based sensing (ABBS) directed to the possibility of a simultaneous multianalyte detection, which would help the system be applied to real analysis. Therefore, we adapted the experimental approach developed for piezoelectric-based sensing to surface plasmon resonance imaging (SPRi), an optical-based sensing technology able to perform high-throughput screenings in real time and without labeling,<sup>9,10</sup> overcoming the limitation of piezoelectric sensing in terms of number of sequences detectable simultaneously. SPRi is considered the most attractive and powerful advancement of conventional SPR. Combining conventional SPR's sensitivity with the spatial capabilities of digital imaging, SPRi currently represents one of the best sensing platforms for the label-free probing of biomolecules in array format. In this work, DNA sequences (i.e., *Cytomegalovirus* promoter (CMV) and Enhanced Green Fluorescent Protein (EGFP) gene, identified as suitable markers of transgenesis,<sup>8</sup>) are detected in human transgenic cells by SPRi. System development is discussed in terms of probe efficiency and influence of secondary structures in hybridization reaction; furthermore, optimization of PCR samples pretreatment to allow their hybridization on biosensors was carried out, together with a strategy to increase SPRi signals *in situ* by molecular architectures for mass enhancement. Real-time PCR (qPCR) was also employed as a reference technique for target analyte detection on human cells (HEK-GFP).

## METHODS AND MATERIALS

**Materials.** 11-Mercapto-1-undecanol (MU), 6-mercapto-1-hexanol (MCH), absolute ethanol, and streptavidin were purchased from Sigma–Aldrich (Milan, Italy). A 184 Silicone Elastomer kit for microwelled polydimethylsiloxane (PDMS) masks was purchased from Dow Corning Corporation (USA). 5'-Biotinylated PCR primers, unmodified ssDNA probes, biotinylated ssDNA probes, and complementary targets were all

purchased from MWG Biotech (Milan, Italy) and are reported in Table 1. Unmodified PCR primers are reported in the work of Scarano et al.<sup>8</sup> Plasmid pEGFP-C1 was from Clontech–Takara Bio Europe (France) and was stably transfected in *E. coli* cells by using a “One Shot TOP10 Chemically Competent” (Invitrogen) kit. For plasmid DNA extraction, NucleoSpinPlasmid kit (Macherey Nagel, MMedical, Florence) was used. Plasmid pEGFP-C1 was quantified at 260 nm by BioPhotometer-Eppendorf (Eppendorf Italia, Milan, Italy). Human embryonic kidney cells (HEK), transfected with the same plasmid (HEK-GFP cells) and the same cell line not transfected (negative control HEK-293) were kindly provided by Prof. A. Arcangeli (Dipartimento di Patologia e Oncologia Sperimentale, University of Florence, Italy). Genomic DNA was extracted from HEK cells according to the instructions of Invisorb Spin Tissue Kit (Invitek, Berlin, Germany). Streptavidin MagneSphere Paramagnetic Particles (SA-PMPs) were purchased from Promega (Milan, Italy) and used according to the supplier's recommendations, unless otherwise specified.

**Buffers and Solutions.** The buffer used for immobilization of thiolated probes was 1 M  $\text{KH}_2\text{PO}_4$ , pH 3.8 (here named Phosphate Acid Solution, PAS). The binding solution (BS) used in SPRi assays was 300 mM NaCl, 20 mM  $\text{Na}_2\text{HPO}_4$ , 0.1 mM EDTA, pH 7.4. All reagents were purchased from Merck (Italy). All solutions were prepared using Milli-Q water and filtered before use by Puradisc syringe filters, cellulose acetate 0.2  $\mu\text{m}$  from Whatman GmbH, Dassel, Germany.

**UV Measurements.** Possible secondary structures on DNA sequences used as probes and targets for biosensor development were investigated by melting experiments conducted on UV–vis Spectrophotometer Cary 100 Bio (Varian, Inc.), interfaced with a computer by a dedicated software (Cary Win UV). Data analysis and fitting was performed using QtiPlot 0.9.7.13. Four micromolar (4  $\mu\text{M}$ ) solutions of each analyzed sequence were subjected to four scans in the temperature range of 12–85 °C (data interval 0.5 °C, scanning rate 1 °C/min) and relative melting profiles acquired (260 nm).

**SPR Imaging Apparatus.** Experiments were conducted on the SPRi-Lab+ produced by Genoptics-Horiba Scientific (Orsay, France). Its optics are based on intensity modulation, measuring the reflectivity variation of a monochromatic incident p-polarized light (635 nm) at a fixed angle. The internal volume of the flow cell is 11  $\mu\text{L}$ . The CCD camera of the instrument has a spatial resolution of  $\sim 40 \mu\text{m}$ . The resonance coupler is a SF-10 glass prism (Genoptics-Horiba Scientific, France) coated with a thin (5-nm) chromium underlayer and 50-nm gold layers. The instrument was completed with a dedicated fluidic, as reported by Scarano et al.<sup>11</sup>

**Probes Array Fabrication.** Arrays of 16 spots were constructed on SF-10 gold prisms by the method previously described in Scarano et al.,<sup>11</sup> in which a thin PDMS layer is used to create microwelled masks for manual probe deposition. Once the mask is positioned on a clean gold layer, thiolated DNA probes at 10  $\mu\text{M}$  were added to wells (800 nL/well) and allowed to react in a moist chamber for 48 h. The PDMS mask then was removed and the prism was immersed in an aqueous solution of mixed thiols (1  $\mu\text{M}$  MCH, 1  $\mu\text{M}$  MU) for 24 h. Finally prisms were rinsed with Milli-Q water and dried under a nitrogen stream. In Figure 1A, on the lefthand side of the figure, a representation of the immobilization scheme utilized for the construction of the array is reported, in which each probe species is defined by a different color (blue for EGFP1, red for EGFP2,

**Table 1. Nucleotidic Sequences of Probes, Targets, and Primers Used in the Work**

Thiolated Probe Sequences (5'–3')	
Thiol EGFP1	HS-(CH <sub>2</sub> ) <sub>6</sub> -GTAGGTGGCATCGCCCTC
Thiol EGFP2	HS-(CH <sub>2</sub> ) <sub>6</sub> -GAAGTTCACCTTGATGCCGT
Thiol CMV	HS-(CH <sub>2</sub> ) <sub>6</sub> -GCCAGGCGGGCCATTACCG
Unmodified Complementary Targets (5'–3')	
EGFP1	GAGGGCGATGCCACCTAC
EGFP2	ACGGCATCAAGGTGAACTTC
CMV	CGGTAAATGGCCCGCCTGGC
Secondary 3' Biotinylated Targets for PCR Samples (5'–3')	
EGFP1_RFBiot3'	GAAGTGTGGCCGTTTACGT-Biotin
EGFP2_RFBiot3'	TGCTTGTCGGCCATGATATA-Biotin
CMV_RFBiot3'	GTCAATAGGGGGCGTACTTG-Biotin
Primer Pairs for Biotinylated PCR (5'–3')	
Biotin-egfp1 Forward	Biot-ACG TAA ACG GCC ACA AGT TC
egfp1 Reverse	CAC ATG AAG CAG CAC GAC TT
Biotin-egfp2 Forward	Biot-TAT ATC ATG GCC GAC AAG CA
egfp2 Reverse	ACA TGG TCC TGC TGG AGT TC
Biotin-cmv Forward	Biot-CAA GTA CGC CCC CTA TTG AC
cmv Reverse	GGC GGA GTT GTT ACG ACA TT

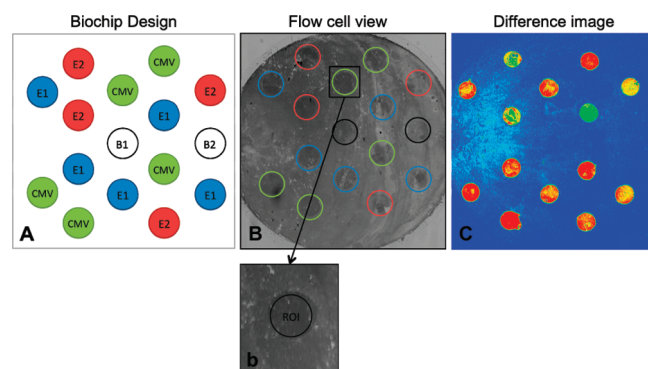


**Figure 1.** (A) Reported representation of biochip design: three probes sets are indicated as E1 (i.e., EGFP1 probe (blue spots)), E2 (i.e., EGFP2 probe (red spots)), and CMV (i.e., CMV probe (green spots)); B1 and B2 are reference spots used as controls. (B) View of the biochip surface into the flow cell through the CCD camera, and representation of signal sampling method: spots of each probe species are separately sampled as ROIs (shown in panel b, beneath the image). (C) Difference image of the biochip after simultaneous binding of all synthetic targets.

and green for CMV). In the middle of the figure (Figure 1B), a view of the biochip surface into the flow cell is visualized through the CCD camera, on which the scheme of SPRi signal sampling method is represented. On the righthand side of the figure (Figure 1C), a difference image of the biochip after simultaneous binding of the three synthetic targets is displayed.

**Signal Sampling on Biochip.** SPRi signals were recorded as changes in percent reflectivity ( $\Delta\%R$ ) versus time (in seconds) and displayed by sensorgrams and difference images in real time by the software SPRi-View L 3.1.0. (Genoptics-Horiba Scientific). Regions of interest (ROIs) were selected by the software at the beginning of the experiment as follows: each receptor spot was sampled and defined as a single ROI (Figure 1b). For each ROI, the recorded  $\Delta\%R$  corresponds to the average of all  $\Delta\%R$  signals recorded for the pixels contained in the ROI.

**SPRi Measurements.** For all measurements, an injection loop of 50  $\mu\text{L}$  was used (Rheodyne). During injections analytes remained in contact with receptors for 10 min for synthetic targets, and 30 min for PCR samples. Excess of unbound analytes were then removed by flowing BS in the flow cell, and SPRi signals sampled when steady state was observed on sensorgrams. Between two cycles of measurements, biochip surface was regenerated with 100 mM HCl in Milli-Q water for 30 s (flow rate 24  $\mu\text{L}/\text{min}$ ). All SPRi experiments were performed at 25  $^{\circ}\text{C}$ .

**Calibration of the Array.** Array of receptors was tested by injecting mixtures of complementary synthetic targets in BS in the range of 1–500 nM. After each measuring cycle, the biosensor surface was regenerated with 100 mM HCl solution for 30 s.

**PCR Samples Preparation.** Unmodified PCR amplicons were amplified from naked plasmid pEGFP-C1 and genomic DNA extracted from HEK cells (HEK-GFP and HEK-293), following Scarano et al.,<sup>8</sup> with the MJ-Research Ptc-200 (Peltier Thermal Cycler) DNA Engine. PCR negative controls contained all PCR reagents other than the DNA template and were always processed with template-containing samples. Moreover, biotinylated sense primers were used, coupled to the relative unmodified reverse primers (see Table 1), to obtain PCR products carrying a biotin residue at their 5' ends and applied in experiments on magnetic separation of the amplicon strands. Amplification protocols were the same as those applied for unmodified PCR

amplicons. PCR amplicons were quantified using PicoGreen (Molecular Probes, Oregon, USA) dye with a TD-700 Fluorimeter (Turner Biosystems, Milan, Italy). PicoGreen was used as fluorescent dye for double-stranded DNA (dsDNA) quantitation in PCR samples,<sup>12</sup> using Lambda Phage DNA (Lambda DNA from Fermentas, Milan, Italy) for fluorimeter calibration in the range of 0–500 ng/mL (concentration of the stock solution 100  $\mu\text{g}/\text{mL}$ ). Dilutions of PCR products were prepared for measurements in TE buffer (10 mM Tris-HCl, 1 mM EDTA, pH 7.5) and spiked with PicoGreen solution to have  $1\times$  final concentration of the dye, respective to the stock solution.

**Real-Time PCR Measurements.** Real-time PCR was performed on ABI Prism 7700 System using the TaqMan technology<sup>13</sup> (Applied Biosystems Group, Milan, Italy), according to the manufacturer's instructions. Standard reference curve was performed in triplicate in 25  $\mu\text{L}$  using 6  $\mu\text{M}$  of each primer, 5  $\mu\text{M}$  of the TaqMan fluorogenic probe (labeled at the 5' end with the JOE Fluorochrome and at the 3' end with the TAMRA quencher),  $1\times$  TaqMan universal Master Mix, 100 ng/tube of the commercial human DNA (Sigma–Aldrich, Milan, Italy) spiked with 1, 5, 25, 50, 100, 200 copies of pEGFP-C1 plasmid. To quantify EGFP target gene in DNA extracted from HEK-GFP and HEK-293 cells, 0.5 ng DNA was added to master mix reaction. As reported in Scarano et al.,<sup>8</sup> to determine the plasmid copy number, we calculated the weight of a DNA plasmid single copy as follows: pEGFP-C1 =  $(4.731 \times 10^3 \times 660)/6.02 \times 10^{23} = 5.19 \times 10^{-6}$  pg. Since the weight of haploid human genomic DNA is 3.75 pg (NCBI), the total number of genome copies contained in 100 ng is 26 667 and, in 0.5 ng, 133 copies. Primers for real time amplification on EGFP gene were 5'-ATCATGGCCGACAAGCAGAAGAAC-3' (forward) and 5'-GTACAGCTCGTCCATGCCGAGAGT-3' (reverse), and the sequence of the internal probe was 5'-CAGCACCATGTGATCGCGCTTCTCGT-3'. Reactions were performed in MicroAmp 96-well plates (Applied Biosystems). Samples were subjected to one cycle of 2 min at 50  $^{\circ}\text{C}$ , one cycle of 10 min at 95  $^{\circ}\text{C}$ , and 50 cycles at 95  $^{\circ}\text{C}$  for 15 s, followed by anneal extension at 60  $^{\circ}\text{C}$  for 1 min.

**Denaturation of PCR Samples.** The denaturation of dsDNA amplicons is necessary for successful hybridization on the biosensor, thus PCR fragments underwent denaturation to obtain single-stranded amplicons (ssDNA), taking two approaches: the thermal denaturation and the magnetic separation of the strands.

**Thermal Denaturation.** PCR samples were denatured by heating at 95  $^{\circ}\text{C}$  for 10 min, followed by a 2 min-treatment at 0  $^{\circ}\text{C}$  in an ice/water bath and then immediately injected in the SPRi flow cell.

**Magnetic Separation.** Streptavidin MagneSphere Paramagnetic Particles (SA-PMPs) coated with streptavidin (average diameter of  $1.0 \pm 0.5 \mu\text{m}$ ) were used for separation of the PCR amplicons containing the target sequences.<sup>14</sup> Here, the protocol that was applied followed the supplier's instructions (Promega Technical Bulletin No. 246). After the neutralization of 100 mM NaOH with 100 mM HCl, the final dilution step, aimed to settle again the initial PCR sample concentration (200 nM), was carried out with two recovery solutions: (1) 1 M Tris-HCl, 100 mM NaCl buffer<sup>14</sup> (SalineTris), and (2) binding solution (BS) used in SPRi assays.

**SPRi Signal Enhancement.** The strategy was applied to ssPCR samples to obtain the enhancement of SPRi signal after their binding on the specific receptor probe. Biotinylated secondary targets carrying biotin at their 3' end (EGFP1\_RFBiot3',



EGFP2\_RFBiot3', and CMV\_RFBiot3', see Table 1) were used to recognize their specific ssDNA amplicon previously bound on the receptor probe. Biotin residues on 3' ends were then exploited to bind streptavidin by one further injection. Its high affinity for biotin ( $K_D = 10^{-14}$  M) ensures a stable and selective binding to biotinylated residues, leading to a mass enhancement and a local change in the refractive index. If some single strand has hybridized the receptor, the further injection of the secondary target, followed by streptavidin, could enhance the recorded signal.

## RESULTS AND DISCUSSION

The detection strategy proposed here is based on the recognition of a transgenic event by targeting suitable DNA sequences of the shuttle vector backbone used in the transgenesis protocol. The CMV promoter sequence and the EGFP marker gene are used here as a fingerprint of the underlying gene doping event. For DNA-based sensing development, here, we have reported the SPRi optimization, in terms of the main analytical parameters, i.e., system selectivity, sensitivity, working range, reproducibility of the measurements, analysis time, sample pretreatment, and possibility to increase SPRi signals by exploiting nucleic/nucleic and biotin/streptavidin specific recognition. Furthermore, attention has been given to discuss possible effects of secondary structures on probes and targets, by UV melting studies, with possible reflection on the analytical performance of the system. Finally, target sequence analysis (EGFP1, EGFP2,

and CMV) on transgenic human cells (HEK-GFP) has been performed using a SPRi-based sensor.

**System Selectivity.** The system was tested for its specificity by injecting the three synthetic targets (EGFP1, EGFP2, and CMV) separately at 500 nM each (see Figure 2 A). Between two measurements, the surface of the biosensor was treated with 100 mM HCl for 30 s to dissociate the probe/target adducts previously formed. The system has proved to be very selective, since each target was bound only to its complementary probe. No significant signal is observed on the noncomplementary probes and reference spots, indicating the absence of undesired nonspecific binding (i.e., cross reactivity) and/or adsorption on the surface. This high selectivity led us to carry out measurements on mixtures of all three targets in one step, enabling simultaneous analysis of different targets in a very short analysis time.

**Evaluation of the Dynamic Range.** To investigate the dynamic range of the biochip, standard solutions in the range of 1–500 nM containing the three complementary targets in binding solution (BS) were injected in the system. In Figure 3, plotted curves obtained during calibration were shown. The reproducibility of measurements was expressed as the coefficient of variation percentage (CV%) averaged on three replicates for each point of concentration, showing values of <10% for all targets. Sensitive signals down to the nanomolar level were recorded, displaying experimental detection limits of 12 nM for EGFP1, 0.2 nM for EGFP2, and 3.5 nM for CMV, respectively. The minimum recordable SPRi signal was considered to be 0.06  $\Delta$ R, which was three times the observed averaged standard deviation (SD) of the baseline (i.e.,  $SD = \pm 0.02 \Delta$ R). The EGFP1 probe/target displayed less sensitivity than EGFP2 and CMV probe/target couples, and this was more evident in the plots showing the linear range obtained for each target and reported in Figure S1 of the Supporting Information. On the other hand, EGFP1 was characterized by the widest dynamic and linear ranges, which reached 250 nM. For EGFP2 and CMV, saturation was obtained at  $\sim 60$  nM. The sensitivity of CMV was the highest among all the tested concentrations. EGFP2 was characterized by the highest slope curve for the range of 0–50 nM. However, a sudden saturation was observed at higher concentrations. Signals corresponding to EGFP2 reached those of EGFP1 at  $\sim 250$  nM (the concentration where all the receptors showed saturation). Although SPRi data and those previously obtained with piezoelectric system<sup>8</sup> were performed under different experimental conditions, it is possible to compare their behaviors and the analytical performances, relative to the two systems. In particular, the experimental detection limits obtained by the SPRi biosensor were  $\sim 1$  order of magnitude lower than those obtained by piezoelectric sensing (i.e., 0.2 nM for EGFP2 and 3.5 for CMV on SPRi, in contrast to 50 nM and 25 nM on piezoelectric, respectively).<sup>8</sup> For EGFP1, we obtained 12 nM on SPRi vs 50 nM obtained by piezoelectric sensing. The low efficiency of EGFP1 was previously evident and explained by the presence of secondary structures on the probe sequence, which could significantly affect the probe/target affinity recognition with significant consequences on the sensor behavior. To elucidate, under the experimental conditions used, if the EGFP1 probe and target can undergo more self-pairing than EGFP2 and CMV, supplementary investigations were carried out by UV measurements in temperature scanning mode.

**Melting Measurements on Probe and Target Sequences.** EGFP1, EGFP2, and CMV sequences, probes and targets, were tested at 260 nm, scanning the temperature from 12 °C to 85 °C.

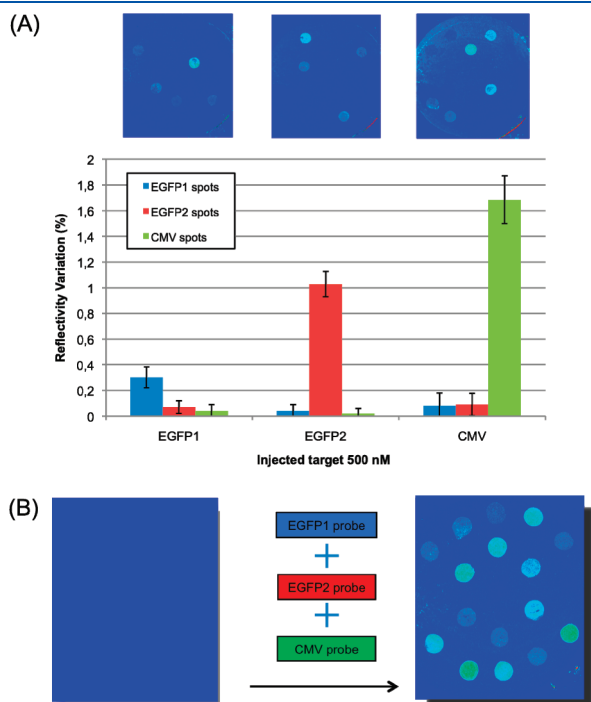


**Figure 2.** (A) EGFP1, EGFP2, and CMV complementary targets were first tested for their specificity toward each corresponding probe sequence (500 nM). Bars report SPRi averaged values with relative standard deviations, calculated on the averaged SPRi values as described in the Methods and Materials section. Regeneration steps among injections were required to recover the probe availability. (B) Representative behavior of the biochip when SPRi measurements were conducted by injecting mixture of all three targets.

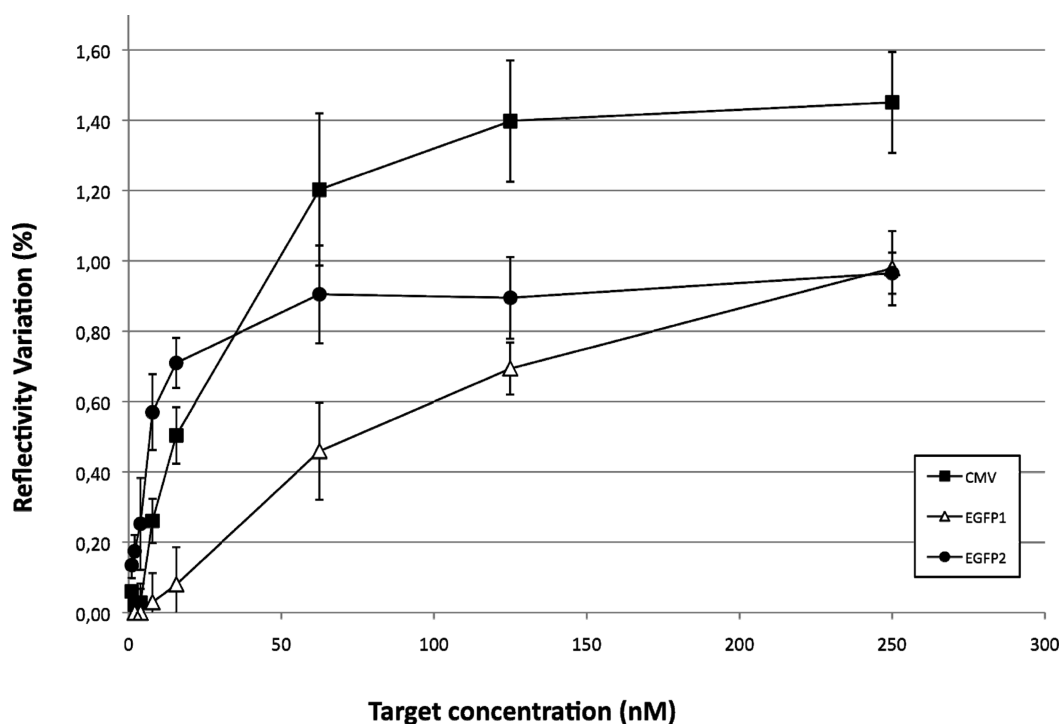


**Figure 3.** SPRi calibration curves with synthetic targets EGFP1, EGFP2 and CMV in the range 1–500 nM. SPRi values are averaged on spots of the same spot species and standard deviations are calculated as described in the Methods and Materials section.

**Table 2.** Melting Temperatures of EGFP1, EGFP2, and CMV Sequences (Probes and Targets)

sequence type	Melting Temperature, $T_m$ (°C)		
	in water	in PAS	in BS
EGFP1-Probe	50	43	62
EGFP2-Probe	14	16	34
CMV-Probe	no melting	no melting	no melting
EGFP1-Target	46		72
EGFP2-Target	22		40
CMV-Target	30 (weak)		53 (weak)

Probe sequences were first tested in Milli-Q water, in phosphate acid solution (PAS), which was used for their immobilization on gold biochips, and in binding solution (BS), which was used as a binding carrier during SPRi assays. Target sequences were tested in Milli-Q water and then in BS. All solutions tested were 4  $\mu$ M in the corresponding diluent. Data collected during melting were fitted with sigmoids and derived as a function of temperature ( $d\text{Abs}/dT$ ) to evidence the  $T_m$  value, at which 50% of double-stranded DNA is denatured.  $T_m$  and relative difference ( $\Delta T_m$ ) values for all samples were reported in Table 2. The CMV probe did not show any melting profile in any of the tested solutions, and CMV target displayed only weak melting profiles both in water and BS. EGFP1 probe and target sequences showed  $\Delta T_m$  values much higher than those displayed by EGFP2 sequences under same conditions. These results supported our findings and explained different probe behaviors: since SPRi experiments were performed at 25 °C, EGFP2 and CMV sequences are presumably more accessible to hybridization than the EGFP1 couple, for which  $T_m$  values are significantly higher than the

working temperature. Probe sequences were tested simulating both immobilization and hybridization conditions, observing that the best unfolding conditions occur in PAS. This confirms previous findings (data not shown), showing that the efficacy of probes is strictly related to specific conditions of the immobilization step, in which the possible presence of hairpins and/or homodimers can influence the self-assembled DNA monolayer during its formation. Therefore, the presence of secondary structures and homodimers could strongly influence both the self-assembled layer formation of the thiolated probe (carried out in PAS), and the availability of the target sequence in BS, affecting the biorecognition efficacy.

**Detection of EGFP by Real-Time PCR.** Real-time PCR was applied as a reference technique to detect the presence of EGFP gene sequence in human genomic DNA samples containing different copies of the plasmid, and in DNA extracted from transgenic cells (i.e., HEK-GFP). The system was calibrated by recording the Ct values for samples spiked with different number of copies of pEGFP-C1 plasmid (1, 5, 25, 50, 100, and 200 copies) in 100 ng/tube of commercial human DNA. Each point of the standard curve (Figure S3 in the Supporting Information) was tested in triplicate. The analyses of 0.5 ng DNA extracted from transgenic (HEK-GFP) and nontransgenic (HEK-293) cells were conducted by using the TaqMan chemistry, with a probe internal to the EGFP gene present in plasmid pEGFP-C1. In the same experiment, 100 ng of human nontransgenic genomic DNA alone (series n.1 of Figure 4) and spiked with different number of copies of the plasmid (series samples 2–7 of Figure 4) were also read as unknown samples as positive controls. DNA from transgenic cells indicated the presence of  $132.01 \pm 9.88$  (SD) copies of EGFP gene per 0.5 ng DNA (series sample 8 of Figure 4, as calculated from the standard curve presented in Figure S3 in the Supporting Information). These findings are in

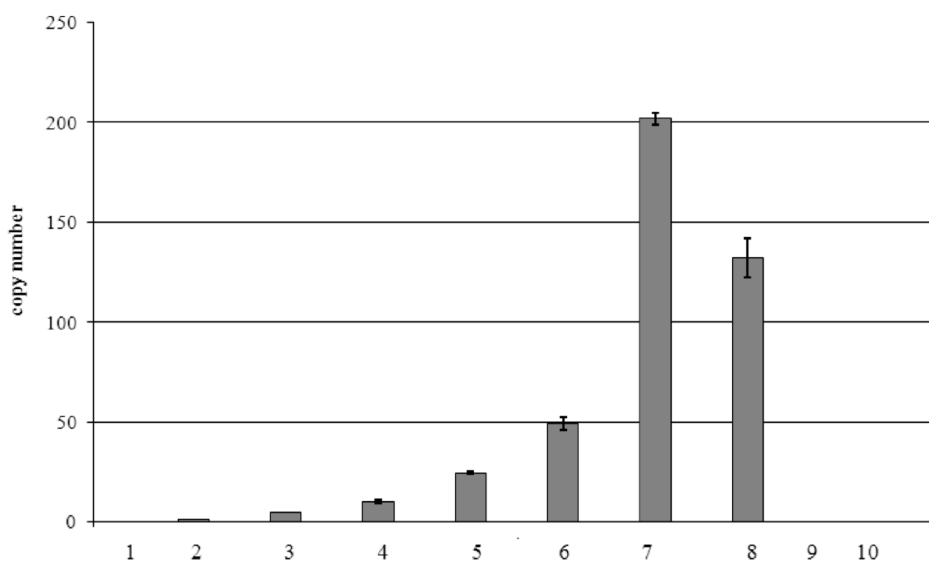


**Figure 4.** Results obtained by real-time PCR on increasing number of pEGFP-C1 copies in human genomic DNA. Sample 1: human genomic DNA alone; samples 2, 3, 4, 5, 6, and 7 correspond to 1, 5, 10, 25, 50, and 200 copies, respectively. Samples 8 and 9 refer to 0.5 ng DNA extracted from HEK-GFP and HEK-293 cells, respectively. Sample 10 is the negative control of the PCR. Each sample was analyzed in triplicate ( $n = 3$ ).

agreement with the expected copy number of 133 copies of haploid genomes, contained in 0.5 ng of tested DNA from transgenic cells. DNA from nontransgenic HEK-293 cells (series sample 9 of Figure 4), tested as negative control, displayed an average value of  $0.29 \pm 0.14$  copies ( $n = 3$ ). Also, the negative control of the PCR (i.e., human genomic DNA alone (series sample 10 of Figure 4)) gave the result of  $0.4 \pm 0.18$  copies ( $n = 3$ ), confirming the absence of nonspecific products.

**Detection of Target Sequences in PCR Samples.** The final objective of the work was the detection by SPRi technique of DNA target sequences in samples amplified by PCR. Thus, after sensor optimization with target synthetic oligonucleotides (EGFP1, EGFP2, and CMV sequences), the system was tested on PCR products obtained using the genomic DNA extracted from transgenic cells (HEK-GFP) as a template, and nontransgenic cells (HEK-293) as a negative control. Three different amplicons containing EGFP1, EGFP2, and CMV target sequences were separately obtained both by using unmodified primers reported in Scarano et al.,<sup>8</sup> and the same primer pairs modified with a biotin residue at the 5' end of each forward primer, as reported in Table 1. Products were quantified by fluorescence, using PicoGreen, and tested at the same concentration (200 nM). Negative PCR samples (all reagents except the template) were also processed to assess nonspecific amplification reactions.

**Sample Pretreatment.** Double-stranded DNA (dsDNA) amplicons were then treated for separating complementary strands to allow further hybridization with corresponding probes. Different protocols are available for denaturing dsDNA, especially focused on DNA sensor development, ranging from simple thermal treatment,<sup>15</sup> dissociation in alkaline conditions with formamide,<sup>16</sup> enzymatic digestion of one strand with exonucleases and separation using magnetic beads,<sup>17,18</sup> and the use of thermal treatment in combination with synthetic oligonucleotides to block renaturation between the strands.<sup>19,20</sup> In all cases, the denaturation breaks hydrogen bonds between complementary bases of the paired strands. Alternatively, also asymmetric PCR<sup>16</sup> was attempted with the intention to directly produce prevalently a single strand during the amplification process.

In this work, different pretreatments to obtain single-stranded PCR samples were evaluated for SPRi application, both on nonmodified and biotin-modified amplicons (see Table 2).

**Thermal Denaturation on Unmodified Amplicons.** Despite simple thermal treatment demonstrated to be suitable for DNA-based sensing in batch-based<sup>17</sup> and in microfluidic-based<sup>15</sup> modes mainly for its simplicity, speed, and low cost, in our case, the easily reversible condition of thermal denaturation did not produce any significant SPRi signal; this was probably due to renaturation of ssDNA during the pathway from the injection loop and the flow cell of the instrument. Our result on SPRi was consistent with previous data obtained for DNA-based biosensors on SPR instrumentation characterized by standard fluidics,<sup>16</sup> despite being refuted by successful data on thermally denatured nonamplified genomic samples tested on SPRi instruments equipped with a microfluidic apparatus.<sup>15</sup> However, in the above cited cases, it was also reported that the sample must be injected as soon as possible ( $\sim 1$  min) after the thermal treatment to avoid its renaturation. Alternatively, PCR products were treated with 1  $\mu$ M of each relative primer pair during the thermal treatment, followed by an annealing step to hybridize primer sequences to the proper ssDNA strands and help them to remain separated in solution.<sup>20</sup> PCR products were then injected and tested, but this method also demonstrated no binding reaction.

**Denaturation of Biotinylated Amplicons by Paramagnetic Microbeads.** Forward primers biotinylated at the 5' end (Table 1) were used for applying sample pretreatment with magnetic microbeads coated with streptavidin. The biotinylated amplicon bound the microbeads surface through streptavidin/biotin recognition.<sup>14</sup> Biotin modification was performed on the primer such that biotin was attached to the strand complementary to the target strand, which was later removed during the treatment with microbeads, while the unmodified one was injected as the target strand. Streptavidin-modified paramagnetic microbeads (SA-PMPs) can bind double-stranded biotinylated amplicons.<sup>14,17</sup> By increasing the pH of the solution, dsPCR dissociation was achieved with a consequent release of the ssDNA target sequence into the supernatant. Magnetic particles carrying



the complementary biotinylated single-stranded amplicons were then separated, using a magnetic field. The supernatant solution contained only the ssDNA target analyte, which was finally neutralized and injected in the system to allow hybridization reaction.

The procedure was applied to 200 nM PCR amplicons (containing the target sequences, i.e., EGFP1, EGFP2, and CMV) obtained following EGFP1-, EGFP2-, and CMV-specific PCR using DNA from transgenic HEK-GFP cells or, as negative control, HEK-293 cells. The relative supernatant solutions containing free single strands of one of the three sequences were then tested on the SPRi chip. The procedure involving SalineTris<sup>17</sup> as the recover buffer led to ssDNA amplicons not being able to hybridize on the chip. In contrast, when the final dilution of ssDNA amplicons is performed in BS, we obtained reliable SPRi signals. The influence of the recovery buffer on the hybridization behavior was assessed in parallel on synthetic oligonucleotides, by testing them in both diluted SalineTris and BS; it was confirmed that the absence of hybridization on ssDNA amplicons was due to the use of SalineTris. In fact, also synthetic targets showed negligible binding when diluted in the SalineTris buffer, but not when diluted in BS, in which SPRi signals were in agreement with sensor calibration (data not shown). This finding justified further use of the BS buffer for the recovery step of SA-PMPs protocol.

**Detection of Transgenic DNA by SPRi.** PCR amplicons were obtained by amplifying specific sequences belonging to the EGFP gene and the CMV promoter of the plasmid pEGFP-C1.<sup>8</sup> In particular, two different amplicons were relative to the EGFP gene, namely, EGFP1 and EGFP2, each carrying the corresponding target sequence; the third amplicon contained the CMV target sequence. Genomic DNA from HEK-293 was used

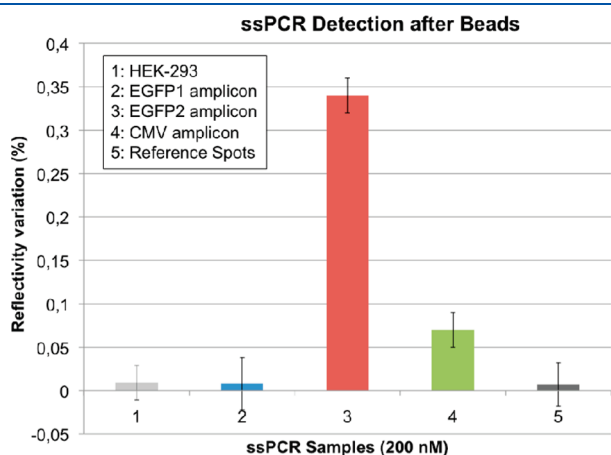


**Figure 5.** SPRi results obtained with 200 nM biotinylated amplicons after strands separation with microbeads. Samples were injected separately and were (from left to right) the result on genomic DNA from (1) HEK-293 cells amplified using the three couples of primers (the responses are averaged on the three amplicons obtained with EGFP1, EGFP2, and CMV primer couples); (2) HEK-GFP cells amplified with EGFP1 primer pair to obtain the amplicon containing the EGFP1 target sequence and tested on the EGFP1 probe; (3) HEK-GFP cells amplified with EGFP2 primer pair to obtain the amplicon containing the EGFP2 target sequence, and tested on EGFP2 probe; (4) HEK-GFP cells amplified with CMV primers couple to obtain the amplicon containing the CMV target sequence, and tested on CMV probe; and (5) response averaged on the two reference spots (Blank1 and Blank2 of the chip) for all amplicons tested.

as negative control and subjected to amplification by preparing three PCR mixtures, each containing the primer couple specific for each target. Each amplicon obtained by PCR was then subjected to the treatment with paramagnetic microbeads to separate the double strands. ssDNA samples obtained from PCR amplicons were separately injected, and SPRi results are showed in Figure 5. Amplicons from HEK-293 DNA were injected as negative controls, since none of the three target sequences must have been amplified. Results confirmed the absence of amplicons, giving an average signal of  $0.009 \pm 0.02 \Delta\%R$  ( $n = 3$ ). The ssDNA from EGFP1 amplicon led to negligible results ( $0.008 \pm 0.02 \Delta\%R$ ,  $n = 3$ ), and this may be directly related to what was evidenced by melting experiments (i.e., the possibility of strong intramolecular folding affecting the biorecognition between probe and target). This demonstrates the key importance of probe selection on analytical performances of the biosensor and stresses the necessity of a rational approach in their design.<sup>21</sup> EGFP2 and CMV amplicons from HEK-GFP cells gave reliable and reproducible results (i.e., SPRi signals of  $0.34 \pm 0.02 \Delta\%R$  ( $n = 3$ ) and  $0.07 \pm 0.02 \Delta\%R$  ( $n = 3$ ), respectively). The biorecognition between each single-stranded amplicon and the corresponding probe on the biosensor displayed high specificity in both cases: negligible signals were recorded on the reference spots B1 and B2. Also cross-binding between each amplicon and the other two noncomplementary probes was assessed. However, EGFP2 and CMV amplicons, tested at the same concentration on the biosensor, displayed very different SPRi signals, and this could be caused by a different binding capacity of ssDNA sequences in interacting with their relative probes on the surface. To elucidate this effect, we estimated the most stable folding for all single strands by Mfold Software.<sup>22</sup> The structures and the relative free energy contents (see Figures S4\_1, S4\_2, and S4\_3 in the Supporting Information) were calculated by imposing to the software  $\text{Na}^+ = 0.34 \text{ M}$  and  $25^\circ\text{C}$  as folding conditions. Despite all of the amplicons displaying stem-loop structures, the CMV sequence is almost entirely involved in this type of structure. The strongest intramolecular base pairing of CMV is also evidenced by its calculated free energy (i.e.,  $-42.11 \text{ kcal/mol}$ , versus  $-34.08 \text{ kcal/mol}$  for EGFP1 and  $-29.59 \text{ kcal/mol}$  for EGFP2 sequences). Although the *in silico* evaluation could only partially explain the actual behavior of the probe/ssDNA target couple, we can assume that, in the case of the CMV amplicon, secondary structures are very strong to affect its interaction with the corresponding probe. In this sense, the experimental finding is in agreement with the result obtained on SPRi with this target sequence. Moreover, results on SPRi are in strong agreement with that reported on piezoelectric devices,<sup>8</sup> demonstrating the robustness of the proposed approach. Moreover, the SPRi system showed the possibility to work in label-free multianalyte detection mode, opening new perspective for high-throughput analysis.

**In Situ Enhancement of SPRi Signal.** With the objective of improving SPRi signals recorded on PCR products, we performed experiments of *in situ* mass enhancement. A schematic representation of the strategy is sketched in Figure 6 (left): ssDNA from a PCR amplicon (the primary target) binds the immobilized thiolated probe and a secondary target that carries a biotin residue at the 3' end (see Table 1) is designed to bind the primary target at its free 5' end. The method was first applied to unmodified PCR amplicons to dispel any doubt about the possibility to record SPRi signals after the thermal treatment and, at the same time, to exclude the presence of very low



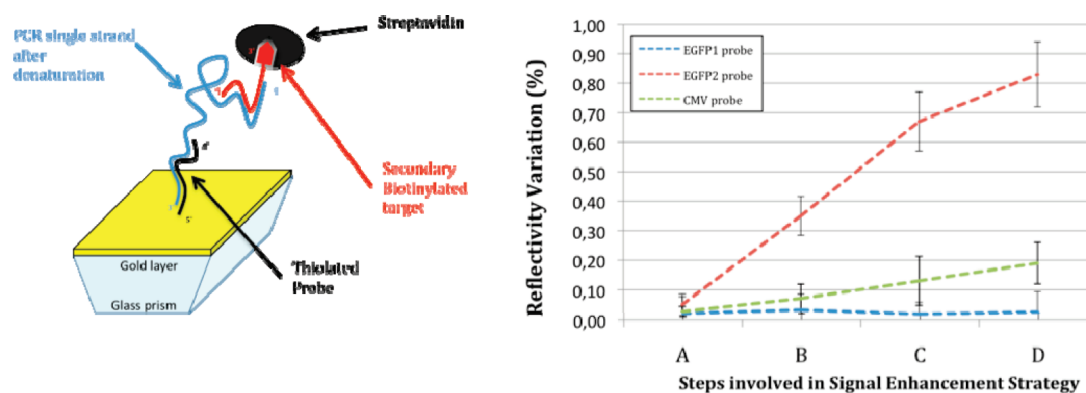


**Figure 6.** Sketched representation of the strategy followed for signal enhancement on PCR amplicons after their denaturation and subsequent binding on biochip (left) and results obtained (right). Legend for the panel on the right side: (A) injection of streptavidin alone; (B) SPRi signals for the three PCR amplicons (200 nM); (C) injection of secondary biotinylated target at equimolar concentration; and (D) streptavidin addition (equimolar to PCR samples) and relative increment of signals.

concentrations of single-stranded amplicons hybridized on the corresponding probe.

Having this objective in mind, after the amplicon has been injected, the 3'-biotinylated secondary target complementary to the corresponding amplicon is injected, followed finally by streptavidin addition. In this case, no reliable SPRi signal was recorded for all amplicons, confirming the hypothesis that the renaturation process of the single strands occurs before that amplicons may reach the measuring cell. In Figure 6 (right), the SPRi signals relative to the steps of the strategy are reported. First, the absence of nonspecific binding of streptavidin on biochip was assessed (A in the right-hand side of Figure 6). The ssPCR sample then was injected (from 200 nM initial sample concentration) and the relative signals were recorded (B in the right-hand side of Figure 6). The specific secondary biotinylated target was injected (C in the right-hand side of Figure 6), and finally streptavidin was added (D in the right-hand side of Figure 6), to enhance the signal. The procedure was performed separately on each ssPCR sample, to assess that no unspecific binding occurred among probe species. Despite the averaged intensities of signals referred to EGFP2 and CMV single-stranded amplicons increased by the addition of the secondary target/streptavidin, we observed a statistically significant increment of the signal only for EGFP2. In the case of EGFP1, no signal enhancement was recorded, confirming the absence of the single-stranded amplicon bound to the relative probe.

These results support the possibility to further develop label-free and selective methods increasing SPRi signals of long DNA sequences bound to the biochip. The approach allowed also distinguishing between DNA targets with low-binding efficiency (CMV) and single-stranded amplicons unable to bind the relative probe (EGFP1) due to structural issues.

## CONCLUSIONS

In this work, we present results and advancements obtained by applying surface plasmon resonance imaging (SPRi) to the development of a high-throughput method for transgenic DNA sequences detection with possible application to gene doping controls. We showed that SPRi technology could be successfully applied to the development of DNA biochips in microarray format for the simultaneous detection of different targets on a single sample. We tested synthetic targets and PCR samples from

human embryonic kidney (HEK) cells transfected with the plasmid pEGFP-C1. The system successfully allowed the detection of specific DNA sequences (EGFP1, EGFP2, and CMV) on the vector backbone in transgenic HEK cells, indicating positive response to the transgenesis event. As a reference method, the EGFP target sequence was analyzed and quantified by real-time PCR. The biosensor's subnanomolar sensitivity was improved, in comparison with previous results obtained on piezoelectric biosensors for the same target analytes.<sup>8</sup> Pretreatments on PCR amplicons, to efficiently denature double helices and promote the hybridization on receptors, were also investigated, obtaining reliable and reproducible results. Finally, a simple strategy for SPRi signal enhancement was presented on PCR products. These results open the possibility to trace transgenic DNA sequences in complex matrices, such as genomic DNA extracts. Our approach focused on vector backbone sequence detection; however, very recently, the direct detection of transgenes has been reported for gene doping controls. In particular, PCR-based protocols for erythropoietin (EPO), or Vascular Endothelial Growth Factor (VEGF) as candidate genes targeting specific recombinant cDNA sequences have been reported.<sup>3</sup> In this sense, a possible extension of our approach should be in the direction of the combination of different probes, by the design of large databases of target sequences (genes, nonviral and viral shuttle constructs, proteins, etc.) suspected of being involved, directly or not, in transgenic protocols for gene doping purposes.

## ASSOCIATED CONTENT

**S Supporting Information.** Additional information as noted in text. This material is available free of charge via the Internet at <http://pubs.acs.org>.

## AUTHOR INFORMATION

### Corresponding Author

\*Tel.: +39 0554573314. Fax: +39 0554573384. E-mail: [minunni@unifi.it](mailto:minunni@unifi.it)

## ACKNOWLEDGMENT

M. Minunni, coordinator of the project "Affinity-Based Biosensing (ABBS) for Gene Doping Detection: A Pilot Study",

would like to thank the World Antidoping Agency (WADA) for funding within the “Scientific Research Grant-2008, Competition topic C: Detection of Prohibited Substances/Methods: novel methodologies”. We also thank Dr. Debora Berti (Dipartimento di Chimica “Ugo Schiff”, Università degli Studi di Firenze, and CSGI) for allowing melting experiments.

## REFERENCES

- (1) Ni, W.; Le Guiner, C.; Gernoux, G.; Penaud-Budloo, M.; Moullier, P.; Snyder, R. O. *Gene Ther.* **2011**, *18*, 709–718 (DOI: 10.1038/gt.2011.19).
- (2) Baoutina, A.; Coldham, T.; Bains, G.; Emslie, K. *Gene Ther.* **2010**, *17* (8), 1022–1032.
- (3) Beiter, T.; Zimmermann, M.; Fragasso, A.; Hudemann, J.; Niess, A. M.; Bitzer, M.; Lauer, U. M.; Simon, P. *Gene Ther.* **2011**, *18*, 225–231.
- (4) Kohler, M.; Thomas, A.; Walpurgis, K.; Schanzer, W.; Thevis, M. *Anal. Bioanal. Chem.* **2010**, *398* (3), 1305–1312.
- (5) Azzazy, H.; Mansour, M.; Christenson, R. *Clin. Biochem.* **2009**, *42* (6), 435–441.
- (6) Minunni, M.; Scarano, S.; Mascini, M. *Trends Biotechnol.* **2008**, *26* (5), 236–243.
- (7) Rogers, K. R.; Mulchandani, A. *Affinity Biosensors: Techniques and Protocols*; Methods in Biotechnology; Humana Press, Inc.: Totowa, NJ, 1998.
- (8) Scarano, S.; Spiriti, M.; Tigli, G.; Bogani, P.; Buiatti, M.; Mascini, M.; Minunni, M. *Anal. Chem.* **2009**, *81* (23), 9571–9577.
- (9) Scarano, S.; Mascini, M.; Turner, A.; Minunni, M. *Biosens. Bioelectron.* **2010**, *25* (5), 957–966.
- (10) Piliarik, M.; Bockova, M.; Homola, J. *Biosens. Bioelectron.* **2010**, *26* (4), 1656–1661.
- (11) Scarano, S.; Scuffi, C.; Mascini, M.; Minunni, M. *Biosens. Bioelectron.* **2010**, *26* (4), 1380–1385.
- (12) Singer, V.; Jones, L.; Yue, S. T.; Haugland, R. *Anal. Biochem.* **1997**, *249* (2), 228–238.
- (13) Heid, C.; Stevens, J.; Livak, K.; Williams, P. *Genome Res.* **1996**, *6* (10), 986–994.
- (14) Mariotti, E.; Minunni, M.; Mascini, M. *Anal. Chim. Acta* **2002**, *453*, 165–172.
- (15) D’agata, R.; Corradini, R.; Ferretti, C.; Zanolì, L.; Gatti, M.; Marchelli, R.; Spoto, G. *Biosens. Bioelectron.* **2010**, *25* (9), 2095–2100.
- (16) Giakoumaki, E.; Minunni, M.; Tombelli, S.; Tothill, I.; Mascini, M.; Bogani, P.; Buiatti, M. *Biosens. Bioelectron.* **2003**, *19* (4), 337–344.
- (17) Mannelli, I.; Minunni, M.; Tombelli, S.; Mascini, M. *Biosens. Bioelectron.* **2003**, *18* (2–3), 129–140.
- (18) Lecaruyer, P.; Mannelli, I.; Courtois, V.; Goossens, M.; Canva, M. *Anal. Chim. Acta* **2006**, *573–574*, 333–340.
- (19) Mannelli, I.; Minunni, M.; Tombelli, S.; Wang, R.; Spiriti, M. M.; Mascini, M. *Bioelectrochemistry* **2005**, *66* (1–2), 129–138.
- (20) Wang, R.; Minunni, M.; Tombelli, S.; Mascini, M. *Biosens. Bioelectron.* **2004**, *20* (3), 598–605.
- (21) Ermini, M. L.; Scarano, S.; Bini, R.; Mascini, M.; Minunni, M. *Biosens. Bioelectron.* **2011**, *26*, 4785–4790.
- (22) Zuker, M. *Nucleic Acids Res.* **2003**, *31* (13), 3406–3415.